

Fork gratings based on ferroelectric liquid crystals

Y. Ma,¹ B. Y. Wei,² L. Y. Shi,¹ A. K. Srivastava,^{1,*} V. G. Chigrinov,¹ H-S. Kwok,¹ W. Hu,² and Y. Q. Lu²

¹State Key Laboratory Advanced Displays and Optoelectronics Technologies, Partner Laboratory in the Hong Kong University of Science and Technology, Clear Water Bay, Kowloon, Hong Kong, China

²National Laboratory of Solid State Microstructures and College of Engineering and Applied Sciences, Nanjing University, Nanjing 210093, China

*abhishek_srivastava_lu@yahoo.co.in

Abstract: In this article, we disclose a fork grating (FG) based on the photo-aligned ferroelectric liquid crystal (FLC). The Digital Micro-mirror Device based system is used as a dynamic photomask to generate different holograms. Because of controlled anchoring energy, the photo alignment process offers optimal conditions for the multi-domain FLC alignment. Two different electro-optical modes namely DIFF/TRANS and DIFF/OFF switchable modes have been proposed where the diffraction can be switched either to no diffraction or to a completely black state, respectively. The FLC FG shows high diffraction efficiency and fast response time of 50 μ s that is relatively faster than existing technologies. Thus, the FLC FG may pave a good foundation toward optical vertices generation and manipulation that could find applications in a variety of devices.

©2016 Optical Society of America

OCIS codes: (050.1950) Diffraction gratings; (050.1960) Diffraction theory; (050.1970) Diffractive optics; (050.2770) Gratings; (050.1940) Diffraction.

References and links

1. J. Verbeeck, H. Tian, and G. Van Tendeloo, "How to manipulate nanoparticles with an electron beam?" *Adv. Mater.* **25**(8), 1114–1117 (2013).
2. L. Allen, M. W. Beijersbergen, R. J. C. Spreeuw, and J. P. Woerdman, "Orbital angular momentum of light and the transformation of Laguerre-Gaussian laser modes," *Phys. Rev. A* **45**(11), 8185–8189 (1992).
3. G. Molina-Terriza, J. P. Torres, and L. Torner, "Twisted photons," *Nat. Phys.* **3**(5), 305–310 (2007).
4. E. G. Abramochkin and V. G. Volostnikov, "Spiral light beams," *Phys. Uspekhi* **47**(12), 1177–1203 (2004).
5. A. M. Yao and M. J. Padgett, "Orbital angular momentum: origins, behavior and applications," *Adv. Opt. Photonics* **3**(2), 161–204 (2011).
6. J. P. Torres and L. Torner, *Twisted Photons: Applications of Light with Orbital Angular Momentum* (John Wiley & Sons, 2011).
7. J. Wang, J. Yang, I. M. Fazal, N. Ahmed, Y. Yan, H. Huang, Y. Ren, Y. Yue, S. Dolinar, M. Tur, and A. E. Willner, "Terabit free-space data transmission employing orbital angular momentum multiplexing," *Nat. Photonics* **6**(7), 488–496 (2012).
8. G. Foo, D. M. Palacios, and G. A. Swartzlander, Jr., "Optical vortex coronagraph," *Opt. Lett.* **30**(24), 3308–3310 (2005).
9. J. Vaughan and D. Willetts, "Interference properties of a light beam having a helical wave surface," *Opt. Commun.* **30**(3), 263–267 (1979).
10. X.-C. Yuan, J. Lin, J. Bu, and R. E. Burge, "Achromatic design for the generation of optical vortices based on radial spiral phase plates," *Opt. Express* **16**(18), 13599–13605 (2008).
11. M. Uchida and A. Tonomura, "Generation of electron beams carrying orbital angular momentum," *Nature* **464**(7289), 737–739 (2010).
12. D. Ganic, X. Gan, M. Gu, M. Hain, S. Somalingam, S. Stankovic, and T. Tschudi, "Generation of doughnut laser beams by use of a liquid-crystal cell with a conversion efficiency near 100%," *Opt. Lett.* **27**(15), 1351–1353 (2002).
13. S. Slussarenko, A. Murauski, T. Du, V. Chigrinov, L. Marrucci, E. Santamato, and E. Santamato, "Tunable liquid crystal q-plates with arbitrary topological charge," *Opt. Express* **19**(5), 4085–4090 (2011).
14. A. V. Carpentier, H. Michinel, Salgueiro, R. José and O. David, "Making optical vortices with computer-generated holograms," *Am. J. Phys.* **76**(10), 916–921 (2008).

15. N. Heckenberg, R. McDuff, C. P. Smith, and A. G. White, "Laser beams with phase singularities," *Opt. Quantum* **24**(9), S951–S962 (1992).
16. Q. Li, *Liquid Crystals Beyond Displays: Chemistry, Physics, and Applications* (John Wiley & Sons, 2012).
17. E. Brasselet, N. Murazawa, H. Misawa, and S. Juodkazis, "Optical vortices from liquid crystal droplets," *Phys. Rev. Lett.* **103**(10), 103903 (2009).
18. Y. Liu, X. W. Sun, D. Luo, and Z. Raszewski, "Generating electrically tunable optical vortices by a liquid crystal cell with patterned electrode," *Appl. Phys. Lett.* **92**(10), 101114 (2008).
19. M. Infusino, A. De Luca, V. Barna, R. Caputo, and C. Umeton, "Periodic and aperiodic liquid crystal-polymer composite structures realized via spatial light modulator direct holography," *Opt. Express* **20**(21), 23138–23143 (2012).
20. N. R. Heckenberg, R. McDuff, C. P. Smith, and A. G. White, "Generation of optical phase singularities by computer-generated holograms," *Opt. Lett.* **17**(3), 221–223 (1992).
21. D. Voloschenko and O. D. Lavrentovich, "Optical vortices generated by dislocations in a cholesteric liquid crystal," *Opt. Lett.* **25**(5), 317–319 (2000).
22. S. J. Ge, W. Ji, G. X. Cui, B. Y. Wei, W. Hu, and Y. Q. Lu, "Fast switchable optical vortex generator based on blue phase liquid crystal fork grating," *Opt. Mater. Express* **4**(12), 2535 (2014).
23. A. K. Srivastava, V. G. Chigrinov, and H.-S. Kwok, "Ferroelectric liquid crystals: Excellent tool for modern displays and photonics," *J. Soc. Inf. Disp.* **23**(6), 253–272 (2015).
24. Y. Ma, S. Jiatong, A. K. Srivastava, Q. Guo, V. G. Chigrinov, and H.-S. Kwok, "Optically rewritable ferroelectric liquid-crystal grating," *Europhys. Lett.* **102**(2), 24005 (2013).
25. A. D. Kiselev, V. G. Chigrinov, and E. P. Pozhidaev, "Switching dynamics of surface stabilized ferroelectric liquid crystal cells: effects of anchoring energy asymmetry," *Phys. Rev. E Stat. Nonlin. Soft Matter Phys.* **75**(6), 061706 (2007).
26. A. K. Srivastava, W. Hu, V. G. Chigrinov, A. D. Kiselev, and Y. Q. Lu, "Fast switchable grating based on orthogonal photo alignments of ferroelectric liquid crystals," *Appl. Phys. Lett.* **101**(3), 031112 (2012).
27. H. Wu, W. Hu, H. C. Hu, X. W. Lin, G. Zhu, J. W. Choi, V. Chigrinov, and Y. Q. Lu, "Arbitrary photo-patterning in liquid crystal alignments using DMD based lithography system," *Opt. Express* **20**(15), 16684–16689 (2012).
28. B. Y. Wei, W. Hu, Y. Ming, F. Xu, S. Rubin, J. G. Wang, V. Chigrinov, and Y. Q. Lu, "Generating switchable and reconfigurable optical vortices via photopatterning of liquid crystals," *Adv. Mater.* **26**(10), 1590–1595 (2014).
29. V. G. Chigrinov, V. M. Kozenkov, and H.-S. Kwok, *Photoalignment of Liquid Crystalline Materials: physics and applications* (John Wiley & Sons, 2008).
30. Q. Guo, A. K. Srivastava, E. P. Pozhidaev, V. G. Chigrinov, and H.-S. Kwok, "Optimization of alignment quality of ferroelectric liquid crystals by controlling anchoring energy," *Appl. Phys. Express* **7**(2), 021701 (2014).
31. A. K. Srivastava, X. Wang, S. Q. Gong, D. Shen, Y. Q. Lu, V. G. Chigrinov, and H. S. Kwok, "Micro-patterned photo-aligned ferroelectric liquid crystal Fresnel zone lens," *Opt. Lett.* **40**(8), 1643–1646 (2015).
32. Y. Ma, L. Y. Shi, A. K. Srivastava, V. G. Chigrinov, and H.-S. Kwok, "Restricted polymer stabilized electrically suppressed helix ferroelectric liquid crystals," in press, *Liq. Cryst.* (2016).

1. Introduction

Optical vortices have attracted attention and have been extensively studied during the past two decades [1–4]. The optical vortex is a light beam characterized by a helical phase front [5]. It can be used for optical tweezers, micro-motors, micro-propellers and have broad applications in the fields of informatics, micromanipulation, and astronomy [6–8]. So far, several techniques have been explored to generate optical vortex [2,9–14]. L. Allen *et al.* have shown that a laser light with a Laguerre-Gaussian amplitude distribution reveals a well-defined orbital angular momentum. An astigmatic optical system may be used to transform a high-order Laguerre-Gaussian mode into a high-order Hermite-Gaussian mode reversibly [2]. In another approach proposed by Yuan *et al.* a multi-element design scheme generates optical vortices of large spectrum width. The key component of the approach is a radially modulated spiral phase plate [10]. Ref. [10] reports the generation of an electron beam with a phase singularity propagating in free space. The interference pattern between the final beam and a plane electron wave in a transmission electron microscope shows the 'Y' like defect pattern characteristic of a beam carrying a phase singularity with a topological charge $m = 1$. All of these approaches are complicated and demand sophisticated setup.

Recently, a very convenient approach for the fabrication of beam vortex is proposed which is based on fork grating (FG) having a diffraction grating with dislocations centered at the beam axis [15]. Some of the fields viz. quantum computing, optical communicating and

micro manipulating demand tunable FG for which liquid crystals (LC) have been used, extensively [13,16,17]. Several methods to generate tunable FG using LCs have been proposed [17–20]. However, the fabrication process is usually too complicated and inconvenient. Besides that, most of the LC material suffers from low optical efficiency and slow switching speed with large driving voltages. Therefore, a new alternative technique for generation of fast switchable and reconfigurable optical vortices with high efficiency is in urgent demand. For the fast switching speed blue phase LC and cholesteric LC with standing helix configuration are very popular [21,22] but the former one requires high driving voltages while the later suffers from limited tune-ability. Another alternative, ferroelectric LC (FLC) because of ultra-fast response times and smaller driving voltages claims to be a potential candidate. FLC has great potential, however, usually FLC show intrinsic diffraction because of the FLC helix and ferroelectric domains and, therefore, it is not possible to exploit them for the photonic elements [23–26]. Recently, a new electro-optical mode called as electrically suppressed helix FLC (ESHFLC) is proposed that does not show intrinsic diffraction and offer high optical contrast [23]. In this work by leveraging the unique optical quality of the ESHFLC and in-plane modulation of the FLC optic axis, we disclose two modes of FG first, DIFF/OFF switchable mode and second, DIFF/TRANS switchable mode by using single-side alignment method. For DIFF/OFF mode grating, it comprises two states i.e. diffraction state (diffractive state forming a diffraction pattern) and OFF state (no light and thus no diffraction pattern). For DIFF/TRANS mode grating, it also involves two states i.e. diffraction state (diffractive state forming a diffraction pattern) and transmission state (light passing through without any diffraction pattern). These gratings can be tuned between these states by applying the alternating electric field. The FLC FG show high diffraction efficiency, fast response time $\sim 50\mu\text{s}$ at $6.67\text{V}/\mu\text{m}$ and high contrast ratio $>1550:1$ at low driving voltage. Therefore, it offers better possibilities for a verity of modern devices.

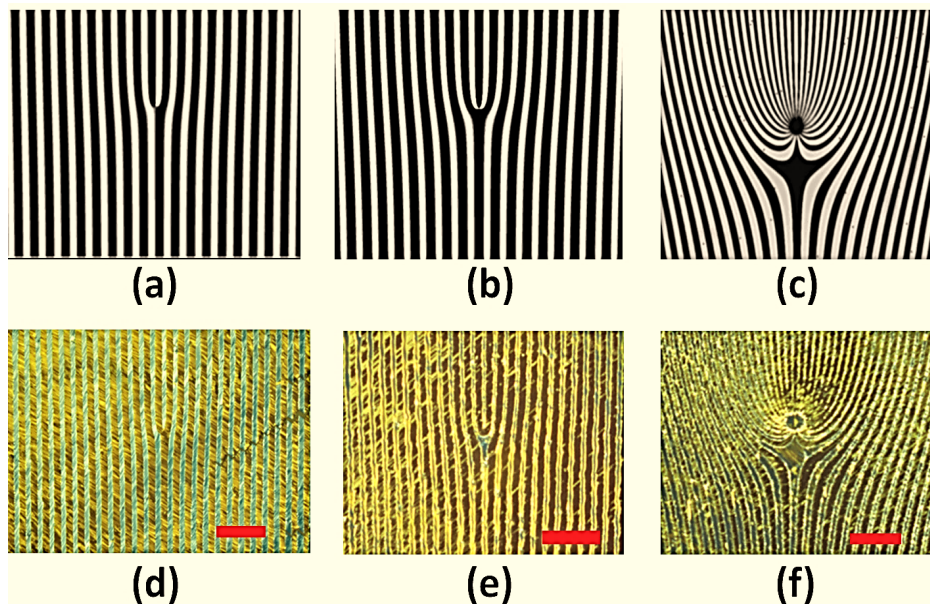


Fig. 1. Computer-generated holograms for (a) $m = 1$, (b) $m = 2$ and (c) $m = 21$. Microphotographs recorded on FLC cells for (d) $m = 1$, (e) $m = 2$ and (f) $m = 21$. The scale bar is $100\mu\text{m}$.

To fabricate the FLC FG a specially designed computer-generated holograms that can convert a Gaussian laser beam into a desired helical mode has been generated by the Digital Micro-mirror Device (DMD) [27]. The DMD generated holograms defines the micro

alignment channels with the distinct easy axis on the photo-alignment surface and so aligns FLC to follow the FG pattern [28]. The interference pattern for the FG pattern can be given by a function [13]:

$$H = |\psi_1 + \psi_2|^2 = |\exp(im\theta) + \exp(ikx)|^2 = 2[1 + \cos(kx - m\theta)]. \quad (1)$$

Here $\theta = \tan^{-1}(y/x)$ is the polar coordinate. The hologram profile can be changed by changing m . Fig. 1 shows the computer-generated hologram plots of H for (a) $m = 1$, (b) $m = 2$ and $m = 21$ respectively that resembles the fork. The patterns carry information of the topological charge m and the reference wave. Afterwards, a glass substrate coated with the sulfonic Azo dye SD1 (Dai-Nippon Ink and Chemicals, Japan (DIC)) has been irradiated by the designed pattern in two steps. The FG micro-pattern comprises two distinct easy axes in the adjacent domains. In the first step of the irradiation, only one of the two substrates of the cell is coated with SD1 and irradiated uniformly with the linearly polarized light to create the uniform alignment. The easy axis of the SD1 can be re-aligned (by another irradiation), thus, to create the two alignment domains the same substrate has been irradiated by the desired computer generated hologram, in the second step [29]. Moreover to create the distinct easy axis in the two alignment domains, the polarization azimuth of the irradiated light has been rotated by some angle. Thus, created alignment domains show distinct easy axes. The different angular combinations of the two easy axes, in the two alignment domains, show different electro-optical modes that have been discussed later in the article. Afterward, the cell has been assembled with the irradiated substrate and a bare ITO substrate [24,25]. The cell gap (d) was maintained at $1.5 \mu\text{m}$ to secure the ESHFLC characteristics.

The microphotographs for the fabricated FG has been shown in Figs. 1 (d), 1(e) and 1(f). The macroscopic texture in each alignment domains resembles with the typical ESHFLC texture with two helical domains [23]. These helical domains transform to the uniform texture in the presence of sufficiently high electric field (typically $\sim 0.5\text{V}/\mu\text{m}$) [23]. The ESHFLC electro-optical mode is characterized by the good alignment quality, high contrast ratio at low driving voltage. It was observed that for the FLC, with pitch (P_o) smaller than the d , shows exceptional optical quality with defect free FLC alignment if the elastic energy of the FLC helix is comparable but obligatory not less than the anchoring energy [23, 24].

The LC used for the present study is FLC FD4004N from DIC having spontaneous polarization $P_s \approx 61 \text{ nC}/\text{cm}^2$ and tilt angle $\theta \approx 22.05^\circ$, which is half of the cone angle (δ). As the ESHFLC mode requires a good control on the anchoring energy for which the SD1 is the most suitable candidate. The anchoring energy of the SD1 films is strongly influenced by the photoinduced ordering and thus depends on the irradiation energy doses [29]. For the chosen FLC for the $d = 1.5 \mu\text{m}$ the optimum anchoring energy is $\sim 4.03 \times 10^{-4} \text{ J}/\text{m}^2$ for which the SD1 layer requires the irradiation energy of $3 \text{ J}/\text{cm}^2$ [24, 29–32]. Thus, all the fabricated cells have been made to meet these critical constraints. However, minor deviations in the desired parameters for the alignment layer and FLC material, in a certain temperature range, does not affect the device performance considerably [30–32].

2. Results and discussion of diffraction model

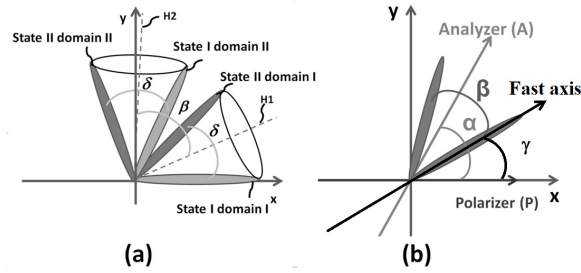


Fig. 2. (a) Illustrates the diagram of FLC molecular orientation in the two states of the two domains, in the x-y coordinate. The angle between the easy axes of the two domains is β . (b) illustrates the positions of the polarizer, analyzer and FLC fast axis. The angle between the polarizer (P) and the analyzer (A) is α and γ represents the angle between the FLC fast axis and the polarizer.

The diffraction profile of thus fabricated FG can be different depending on the phase retardation and mutual orientation of the easy axis in the two domains. Furthermore, the polarization azimuth of the impinging light and the optic axis of the analyzer also plays a crucial role to decide the optical performance. Figure 2(a) illustrates the FLC molecular orientation in the two states of the two domains. These states have been abbreviated as State I Domain I (S_{11}), State I Domain II (S_{12}), State II Domain I (S_{21}), and State II Domain II (S_{22}). The H1 and H2 are the FLC helix axes in the two domains that also represent the alignment directions for two domains.

To study the diffraction profile of the fabricated FG, a square wave electric field has been applied to the ESHFLC FG cell, which was placed between the crossed polarizers. A CCD camera was used to observe the diffraction profile. On the application of the electric field, the P_s follow the electric field and thus the FLC molecules modulate in the two states separated by the cone angle δ . The FLC molecules in domain I, switches between states S_{11} and S_{21} the same is true for the domain II, where the molecule switches between S_{12} and S_{22} . The principle of ESHFLC FG diffraction is based on the different optics (i.e. phase and amplitude) of the light wave passing through the two alignment domains. For one polarity of the applied electric field, the optics of the two domains is the same and, therefore, the light passing through the two domains does not show any diffraction. Although for the other polarity of the applied electric field, the optics of the two domains is different and, as a result, we observe the diffraction. Thus, the diffraction for the ESHFLC FG, in the crossed polarizers, is only limited to one of the polarities of the applied electric field while no diffraction exists for another polarity of the electric field.

The optics of the two different modes can be optimized by considering the E vector of the light passing from different domains in the different state, which can be defined as $E_{i,j}$ where i and j present the state and domain respectively. Thus, depending on the E vector passing through the proposed FG we can define an optimization function (F) as follows [31]:

$$F = \left[(E_{1,1} \cdot E_{1,2} + 1)^2 + (E_{1,1} + E_{1,2})^2 \right] + \left[(E_{2,1} \cdot E_{2,2} - 1)^2 + (E_{2,1} - E_{2,2})^2 \right]. \quad (2)$$

Thus, the two modes of the proposed FG can be described as follows.

2.1 DIFF/OFF Mode

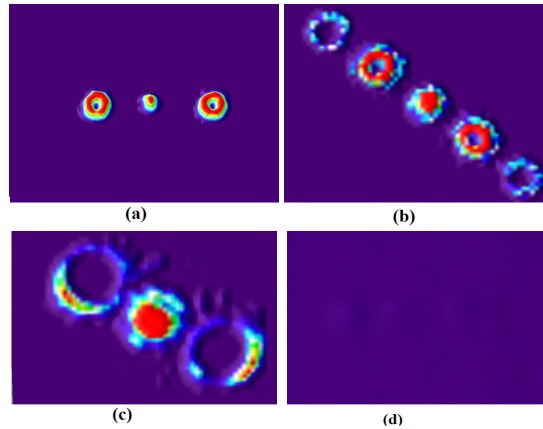


Fig. 3. CCD camera photographs for (a) $m = 1$, (b) $m = 2$ and (c) $m = 21$ for diffraction state and (d) in off state.

Based on Eq. (2) the best angles, for the maximum diffraction efficiency (DE) in the state II and the minimum transmittance in the state I, are $\beta = 90^\circ$, $\gamma = 0^\circ$ and $\alpha = 90^\circ$ [31]. Thus, the proposed FLC FG cell is placed between crossed polarizers such that the polarization azimuth of the impinging light is parallel to a switching position of any one of the two domains. On the application of the square wave electric field, with sufficiently higher magnitude, to the cell, the FLC molecule, in the two domains, modulates and consequently the diffraction also modulates [29].

The diffraction profile for the FG in DIFF/OFF mode has been shown in Fig. 3. The optical vortices are observed in the diffraction orders on both sides of 0th order. The topological charges of these optical vortices are given by nm , where n represents the diffraction order with the highest efficiency. Figure 3(a) is the top view of 0th and ± 1 st orders for the ESHFLC FG with $m = 1$ at the applied voltage of 5V. Figure 3(b) shows the intensity profile for diffraction state of the ESHFLC FG with $m = 2$. Because of the different m , the topology of the ring is different from $m = 1$ and the black hole becomes larger which is even more clear from Fig. 3(c) for $m = 21$. Figure 3(d) represents the off state for all of these FG cells, which is the same for all the cells with different m . From the theoretical model the DE can reach up to 40.5% however, experimentally measured value is 37.8%. The small discrepancy between experimental results and calculation is mainly due to small non-uniformity in the d , the ESHFLC alignment quality and defects boundaries between the two alignment domains. These problems can be easily sorted out by simple optimizations of cell and material parameters [29–32].

2.2 DIFF/TRANS Mode

Another important mode is DIFF/TRANS mode, wherein one state we see the diffraction while in the other state the light passes through without any diffraction. In order to get the maximum diffraction efficiency in the first state and the maximum transmittance in the second state, the Eq. (2) drives the angles as $\beta = 45^\circ$, $\gamma = 67.5^\circ$ and $\alpha = 90^\circ$. Thus within the limits of ESHFLC conditions and angular restrictions defined above we have fabricated an FG with $m = 1$. Afterward, it has been characterized for the diffraction and transitive state in the Fig. 4. Figure 4(a) and 4(c) show the diffraction and transmission state respectively. The DE is $\sim 38\%$ and transmittance in the transmission state is over 95%, which is very close to the theoretically calculated values.

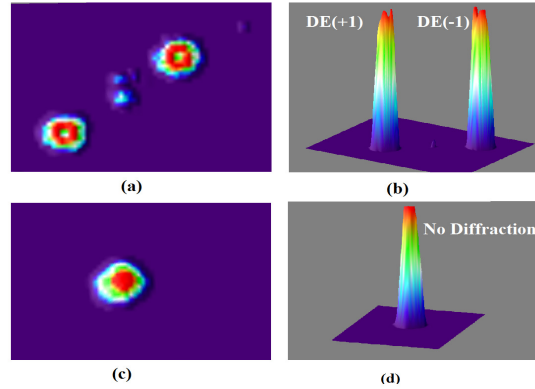


Fig. 4. CCD camera photographs for the FG, with $m = 1$ and the optimization conditions defined above, for top (a) and front view (b) in diffraction state and the transmission state of top (c) and front view (d).

The contrast ratio (CR) and switching time are also important parameters for the proposed FG. The CR for the $\pm 1^{\text{st}}$ order diffraction (i.e. $CR = I_{Max} / I_{Min}$) is $\sim 1500:1$ for the both operational modes. It is not the optimum and further optimization of the anchoring energy and cell parameters can improve the CR and DE, significantly [30]. The switching time of the ESHFLC with rotational viscosity γ_{ϕ} is given by $\tau = \gamma_{\phi} d / P_s V$ [22]. At the applied voltage of 10V, the τ for both switching ON and switching OFF is $\sim 50 \mu\text{s}$. Such a fast τ enables us to drive the device up to very high driving frequency up to $f \cong 2 \text{ kHz}$ with evidently saturated optical states [24]. The proposed FG reveals a $\tau \sim 160 \mu\text{s}$ even at a smaller electric field of $2 \text{ V}/\mu\text{m}$ that decreases to $50 \mu\text{s}$ at electric field of $6.67 \text{ V}/\mu\text{m}$.

3. Conclusion

In conclusion, we have demonstrated the switchable photo-aligned ESHFLC FG structures by utilizing a DMD based microlithography system. Two modes are revealed: DIFF/OFF and DIFF/TRANS switchable mode. The proposed two modes are characterized by small τ and high DE at the small electric field. The τ of $50 \mu\text{s}$ at $6.67 \text{ V}/\mu\text{m}$ has been achieved with the first order CR $\sim 1500:1$. Thus, the proposed diffracting structure shows good optical quality fast electro-optical modulations at the cost of low power consumption, which is much faster than the existing alternatives. The device performance could be improved further by the proper selection of optimized FLC material and photo-alignment parameters. Therefore, the ESHFLC FG, with exceptional optical quality and easy fabrication process, has great potential to find applications in many modern devices.

Acknowledgments

The support by the Hong Kong Government Innovation and Technology Fund, the National Natural Science Foundation of China (NSFC) programs (Nos. 61490714 and 61575093), the State Key Laboratory on Advanced Displays and Optoelectronics Technologies (Project No: ITC-PSKL 12EG02), the Open Foundation Project of National Laboratory of Solid State Microstructures and Hong Kong SAR Research Grants Council grant number 614413 are greatly acknowledged.